Virtual Electrode–Induced Phase Singularity
A Basic Mechanism of Defibrillation Failure

Igor R. Efimov, Yuanna Cheng, David R. Van Wagoner, Todor Mazgalev, Patrick J. Tchou

Abstract—Delivery of a strong electric shock to the heart remains the only effective therapy against ventricular fibrillation. Despite significant improvements in implantable cardioverter defibrillator (ICD) therapy, the fundamental mechanisms of defibrillation remain poorly understood. We have recently demonstrated that a monophasic defibrillation shock produces a highly nonuniform epicardial polarization pattern, referred to as a virtual electrode pattern (VEP). The VEP consists of large adjacent areas of strong positive and negative polarization. We sought to determine whether the VEP may be responsible for defibrillation failure by creating dispersion of postshock repolarization and reentry. Truncated exponential biphasic and monophasic shocks were delivered from a bipolar ICD lead in Langendorff-perfused rabbit hearts. Epicardial electrical activity was mapped during and after defibrillation shocks and shocks applied at the plateau phase of a normal action potential produced by ventricular pacing. A high-resolution fluorescence mapping system with 256 recording sites and a voltage-sensitive dye were used. Biphasic shocks with a weak second phase (<20% leading-edge voltage of the second phase with respect to the leading-edge voltage of the first phase) produced VEPs similar to monophasic shocks. Biphasic shocks with a strong second phase (>70%) produced VEPs of reversed polarity. Both of these waveforms resulted in extra beats and arrhythmias. However, biphasic waveforms with intermediate second-phase voltages (20% to 70% of first-phase voltage) produced no VEP, because of an asymmetric reversal of the first-phase polarization. Therefore, there was no substrate for postshock dispersion of repolarization. Shocks producing strong VEPs resulted in postshock reentrant arrhythmias via a mechanism of phase singularity. Points of phase singularity were created by the shock in the intersection of areas of positive, negative, and no polarization, which were set by the shock to excited, excitable, and refractory states, respectively. Shock-induced VEPs may reinduce arrhythmias via a phase-singularity mechanism. Strong shocks may overcome the preshock electrical activity and create phase singularities, regardless of the preshock phase distribution. Optimal defibrillation waveforms did not produce VEPs because of an asymmetric effect of phase reversal on membrane polarization. **(*Circ Res*. 1998;82:918-925.)**

Key Words: implantable cardioverter defibrillator ■ mechanism of defibrillation ■ defibrillation waveform ■ optical imaging ■ voltage-sensitive dye

It was shown a century ago that a strong electric shock can stop VF in dogs.[1] Fifty years later, it was confirmed in humans in open-chest[2] and transthoracic[3] defibrillation. In 1970, the idea of an automatic ICD was proposed.[4,5] The recent clinical success of the ICD has been primarily driven by purely empirical studies. Despite significant research efforts, the basic mechanisms of defibrillation are not fully understood. Systematic investigation of the effects of strong electric shocks on the heart has been difficult, mostly because of the presence of shock-induced artifacts in any recordings obtained with conventional (electrical) electrophysiological recording techniques. These artifacts make it impossible to record for periods of up to tens of milliseconds after the shock. The recent application of fluorescent methods with voltage-sensitive dyes to cardiac electrophysiology has finally delivered a technique capable of recording transmembrane voltage changes during shocks that are free of electrical artifacts. These recordings can be obtained from a single site,[6] from several sites,[7] and from several hundred recording sites simultaneously.[8]

We recently demonstrated that a monophasic defibrillation shock delivered from an internal defibrillation electrode produces an epicardial transmembrane polarization arranged in a heterogeneous polarity-dependent pattern, described as a VEP.[8] An anodal 10-ms shock, for instance, creates an area of negative polarization near the electrode and two areas of positive polarization on either side. A cathodal shock produced a similar pattern, but of opposite polarity. We have also demonstrated that after shock withdrawal, depolarization spread from depolarized to negatively polarized areas. We hypothesized that this heterogeneity in polarization and the subsequent spread of depolarization might be responsible for the failure of the shock to defibrillate, by creating the substrate for postshock dispersion of repolarization and reentry.

In 1946, Wiener and Rosenblueth[9] proposed a mechanism by which a reentry can be induced. They predicted "the

Received January 29, 1998; accepted March 16, 1998.
From the Department of Cardiology, Cleveland Clinic Foundation, Cleveland, Ohio.
Correspondence to Igor R. Efimov, PhD, Department of Cardiology/Desk FF1, Cleveland Clinic Foundation, 9500 Euclid Ave, Cleveland, OH 44195. E-mail efimovi@cesmtp.ccf.org

Selected Abbreviations and Acronyms

AP = action potential
CM = critical mass
ICD = implantable cardioverter-defibrillator
LV, RV = left and right ventricle
ULV = upper limit of vulnerability
VEP = virtual electrode pattern
VF = ventricular fibrillation

initiation of a one-way wave by successive stimulation of two overlapping small regions of two dimensional system," (Reference 9, page 219, Figure 5) which may lead to a pattern of electrical activity similar to what is known now as a figure-8 reentry. This mechanism has been carefully explored both theoretically and in the chemical Belousov-Zhabotinsky reaction by Winfree,[10] who recognized in this electrophysiological mechanism the abstract concept of a *point of singularity*, which has long been known in physics and mathematics. The experimental protocol of inducing the point of singularity qualitatively similar to that of Wiener and Rosenblueth[9] was first successfully applied in the heart by Frazier et al,[11] who named this protocol *cross-field stimulation*, and the point of singularity was named by them *the critical point*. We will refer to the cross-field stimulation for inducing critical points[11] as *the critical-point mechanism*.

As pointed out by Winfree,[10] a functional reentrant circuit presents an example of an abstract concept known in mathematics as a point of singularity. In fact, this is the only known example of this concept in electrophysiology. The term singularity refers to the impossibility of defining a value of a function at some unique point. The electrical activity of cardiac muscle can be described in terms of phase (ϕ), with $\phi=0$ being assigned to the onset of an AP and $\phi=2\pi$ assigned to the fully repolarized state. In two dimensions, a point of phase singularity is defined as a point in which the following is true: $\oint_{L\to 0}\vec{\nabla}\phi\cdot d\vec{l}\neq 0$, where $L=\oint|d\vec{l}|$. We hypothesized that the VEP may contain a point that is surrounded by positively polarized (excited), nonpolarized (refractory), and negatively polarized (excitable) areas. Therefore, the phase in such a point will yield the above equation, and this point of phase singularity may be responsible for the initiation of reentrant activity.

We have therefore investigated the role of these mechanisms in the defibrillation process using a 256-site fluorescent recording system.

Materials and Methods

Langendorff-perfused rabbit hearts (n=12) were used in the present study. Detailed protocols have been previously published[8] and will be only briefly described. The intact heart stained with di-4-ANEPPS (Molecular Probes) was perfused via the aorta and kept in a temperature-controlled bath containing 15 mmol/L butanedione monoxime to avoid motion artifacts. Figure 1 shows the heart as it was seen by the imaging system. The red square in the left panel shows a typical field of view, which could be readjusted from 3×3 to 25×25 mm. The heart was stimulated by a bipolar electrode sutured to the LV apex at a basic cycle length of 300 ms. Shocks (n=202, 16.8±8 per heart) were delivered during the plateau phase of the ventricular AP by a clinical defibrillator (HVS-02, Ventritex) between the two modified coil electrodes (4007L, Angeion) shown in gray: one 9-mm coil inside of the RV and another 6-cm coil floating above the heart in the perfusate. Different shock waveforms were used (see Figure 1): in each, the first phase had a leading-edge voltage of 100 V, whereas the leading-edge voltage of the second phase was always of the opposite polarity and varied from 0 to 200 V. The duration of each phase was 8 ms. Nearly half of the shocks (55.4%, 112 of 202) resulted in extra beats, ventricular tachycardia, and/or ventricular fibrillation. Sustained episodes of VF were defibrillated with either monophasic or biphasic shocks. Both successful (n=12) and failed (n=19) defibrillation shocks were analyzed. The timing of shock delivery was set as previously described[8]: a mean activation time was defined in the field of view during basic cycle length activation, and then the S_1S_2 coupling interval for the shock application was set to occur at a 50- or 100-ms delay from the mean activation time.

Fluorescence was excited by a semimonochromatic light source (520±45 nm) and collected at >610 nm by a 16×16 photodiode array (C4675, Hamamatsu). Optical signals were amplified, filtered at 1 kHz, and sampled at a rate of 2 kHz with 12-bit resolution. Two hundred fifty-six high-quality optical recordings (peak-to-peak signal-to-noise ratio, 52±14 [mean±SD]; 12 hearts×256 recordings) were acquired, in addition to conventional ECG records, aortic pressure traces, and the pacing and shock hardware triggers that were acquired for documentation and signal analysis purposes.

Data processing included several previously described computer algorithms implemented in software, developed by Igor Efimov, based on the LabVIEW environment (National Instruments). These algorithms automatically calculated activation,[12] repolarization,[13] and shock-induced polarization[8] maps, which were displayed as gray-scale plots. Final publication quality color plots were produced using Origin 5.0 graphing software (Microcal Software).

Activation maps were reconstructed using a $-(dF/dt)_{max}$ algorithm.[12] This algorithm finds the maximum of the first derivative of the inverted fluorescence intensity ($-dF/dt$). The time of $-(dF/dt)_{max}$ was considered as the activation time point at the recording site from which the signal was acquired. Repolarization was calculated from the second derivative of the inverted fluorescence signal intensity and by locating the local maximum peak $-(d^2F/dt^2)_{max}$, which corresponds to the repolarization time point at the recording site.[13] Shock-induced polarization was calculated by subtracting signals recorded during the last basic beat APs from the signals acquired during the shock application.[8] Since the fluorescence signal cannot be absolutely calibrated with respect to the millivolt value of transmembrane voltage, we used a pseudo-millivolt calibration, based on the assumption that the normal AP recorded from every site has a 100-mV amplitude and a −85-mV resting potential.

Results

Figure 1 shows representative superimposed recordings from one of 256 recording sites (black square in left panel). Figure 2 shows a representative map of APs recorded from all 256 recording sites during a basic beat, superimposed with a recording during a shock (+100/−50 V) applied at the plateau phase of the ventricular AP.

The right panels of Figure 1 show superimposed optical recordings performed during 10 basic beats (control APs) and 10 applications of different waveforms for anodal (upper panel) and cathodal (lower panel) shocks, respectively. These recordings demonstrate that the recording site underwent either positive (upper) or negative (lower) polarization during the first phase of the shock relative to the preshock transmembrane potential. The magnitude of the polarization depended on both the polarity of the shock and the location of the recording site (see Figures 2 and 3). Spatially, the polarization produced by the first phase was arranged in the VEP similar to our data reported for monophasic waveforms.[8]

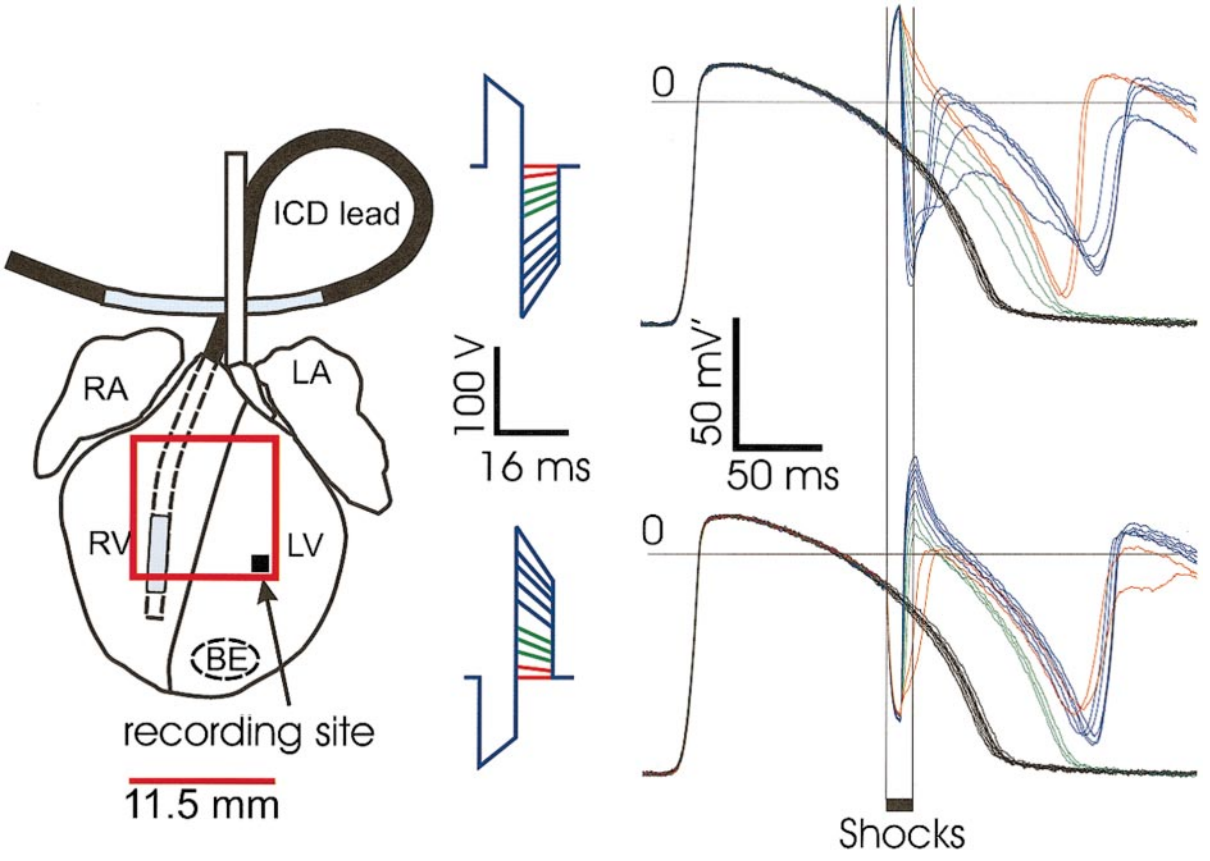

Figure 1. Experimental techniques and optical recordings. Langendorff-perfused rabbit hearts were paced at a basic cycle length of 300 ms by a bipolar electrode (BE) sutured to the LV apex. Biphasic shocks of different polarity were applied during the plateau phase of an AP. Shock waveforms are shown in the upper middle (anodal) and lower middle (cathodal) panels. The first phase of each shock was 100 V in amplitude; the second phase was varied (range, from 0 to 200 V). The upper right and lower right panels show 10 superimposed recordings during the last basic beat and 10 recordings during the application of shocks. The timing of the 16-ms shock application is shown with the black bar and two vertical lines. Transmembrane voltage was calibrated on the basis of the assumption of a 100-mV control AP amplitude and a −85-mV resting potential. On the left, a single recording site (solid black box) out of 256 (red square) is shown. RA and LA indicate right and left atrium, respectively.

The second phase of the shock partially or fully reversed the polarization produced by the first phase in every recording site, in an amplitude-dependent fashion, for either shock polarity. However, there was a striking difference in the reversal of polarization, depending on the sign of the polarization produced by the first phase. In this example, >70 V was required to fully reverse the positive polarization (blue upper traces, Figure 1), whereas only ≥20 V was required to reverse the negative polarization (green and blue lower traces, Figure 1). Therefore, waveforms with a second-phase leading-edge voltage between 20 and 70 V (green traces in both upper and lower panels, Figure 1) produced a positive polarization nearly everywhere throughout the field of view (middle map, Figure 3). Waveforms with a second-phase leading-edge voltage either weaker than 20 V or stronger than 70 V created a highly heterogeneous polarization pattern, with the simultaneous occurrence of positive (red) and negative (blue) polarizations (left and right maps, Figure 3). Furthermore, as seen in Figures 1 and 2, shocks with a second-phase leading-edge voltage between 20 and 70 V resulted in no postshock evoked responses, whereas every other shock initiated postshock extra beats or sustained VF (see examples in Figures 4 and 5, respectively).

We reconstructed isochronal activation maps of postshock beats resulting from VEPs by using the $-(dF/dt)_{max}$ technique.[13] Figure 4 shows a typical pattern of activation and selected optical recordings of a postshock reentrant beat. This pattern of activation was reproduced in all 12 hearts. The upper left panel shows the transmembrane voltage distribution at the end of a +100/−200-V biphasic shock, applied during the plateau phase of an AP. The area of the recordings and the location of the electrodes were the same as in Figure 1 (red box). Tissue located close to the electrode underwent a strong depolarization, which decreased with distance from the electrode in the superior direction (red, Figure 4), whereas the lateral area underwent negative polarization (blue, Figure 4), which also decreased in the superior direction. The circle (Figure 4) indicates a point of shock-induced phase singularity.

Tissue in the lower left quadrant of the field of view was strongly depolarized, whereas the tissue in the lower right quadrant was negatively polarized, restoring excitability in that area. As shown in the eight superimposed optical recordings in the lower left corner of Figure 4, the depolarized area excited the negatively polarized areas (see red arrow and corresponding traces). First, this excitation was transmitted electrotonically, via a mechanism

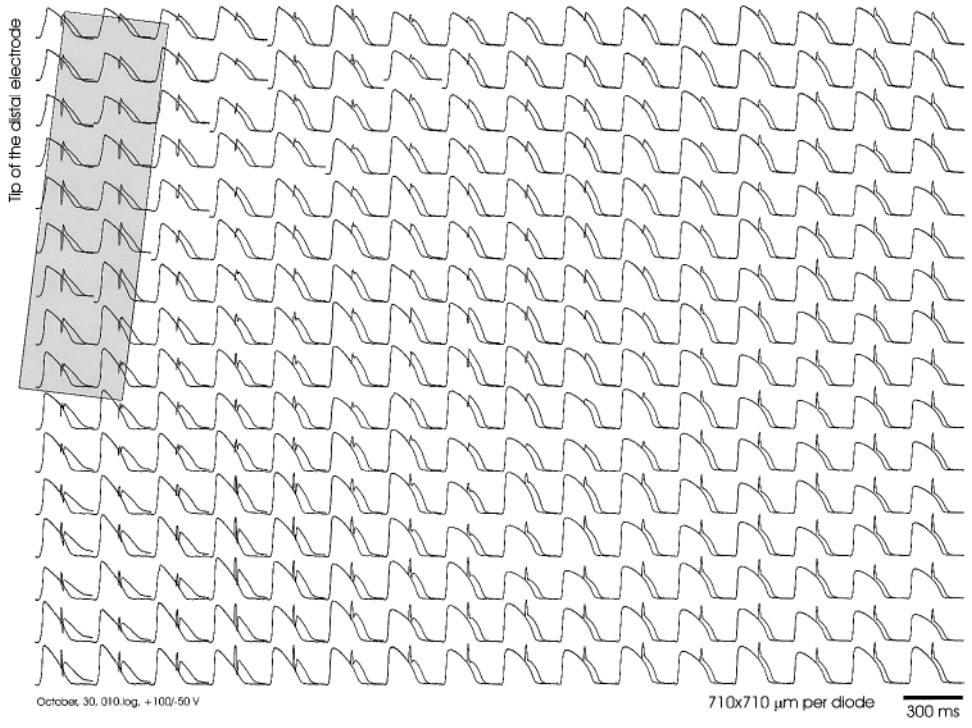

Figure 2. Two superimposed maps of 256 optical APs recorded from the anterior ventricular epicardium during normal rhythm and during application of a truncated exponential biphasic shock (+100/−50 V [8 ms/8 ms], 200-μs delay between phases, and 150-μF capacitor). The average signal-to-noise ratio of this recording was 47±15 (mean±SD, n=256). Optical recordings were obtained from the 11.5 mm×11.5 mm area of epicardium indicated by the red box in Figure 1. Each signal was recorded from an area of 710×710 μm. The shaded rectangle indicates the position of the distal defibrillation electrode.

similar to the "break" excitation described by Roth,[14] through the narrow isthmus between the areas that were strongly negatively polarized and those that were strongly depolarized (slow-rising, low-amplitude, decaying responses in the first four red traces in the postshock time window). This functional isthmus was formed by cells that were put into different phases of refractoriness by the shock. Thus, the electrotonus first activated the excitable negatively polarized area (presumably containing reactivated sodium channels), resulting in fast propagation with full-amplitude APs (last four black recordings).

At the same time, the upper half of the field of view demonstrated unidirectional conduction block in the left-to-right direction (thick black line in the upper middle panel). The lower driving force provided by the upper left depolarized area was unable to activate the less negatively polarized area in the upper right panel. Activation in this area followed the restoration of the resting potential from the lower right area (see blue arrow in traces in lower right and upper middle panels). The upper right panel demonstrates the continuation of the reentrant activity, from right to left, in the upper half of the field of view. In addition, as seen in the lower right corner of this panel, an additional activation wave front spread from an area below the field of view. This indicates that additional phase singularities may have been induced by the shock in areas beyond our field of view.

Figure 5 presents postshock maps of activation recorded from a field of view (15.5 mm×15.5 mm) larger than that in Figure 4. The maps in the lower middle and right panels demonstrate that, indeed, there are two reentrant circuits formed at one side from the electrode. This finding was observed in both of two different experiments performed with a larger field of view (15.5×15.5 mm) after a total of five shocks.

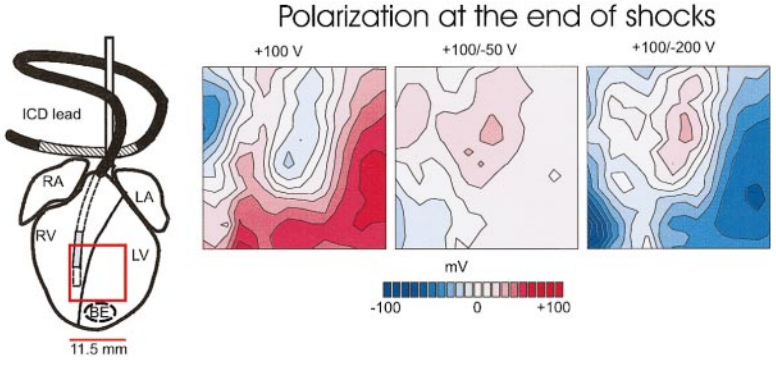

Figure 3. The spatial pattern of polarization at the end of the shock produced by a monophasic shock (+100 V, 7th ms of an 8-ms shock), optimal biphasic shock (+100/−50 V, 15th ms of 16-ms shock), and nonoptimal biphasic shock (+100/−200 V, 15th ms of 16-ms shock). Figure 2 shows the data used for calculating the middle map of this figure. The area of recordings (11.5 mm×11.5 mm) is shown by the red box. Values of polarization are shown relative to the preshock transmembrane voltage, with red assigned to positive polarization, blue to negative polarization, and white to areas of no polarization. RA and LA indicate right and left atrium, respectively; BE, bipolar electrode.

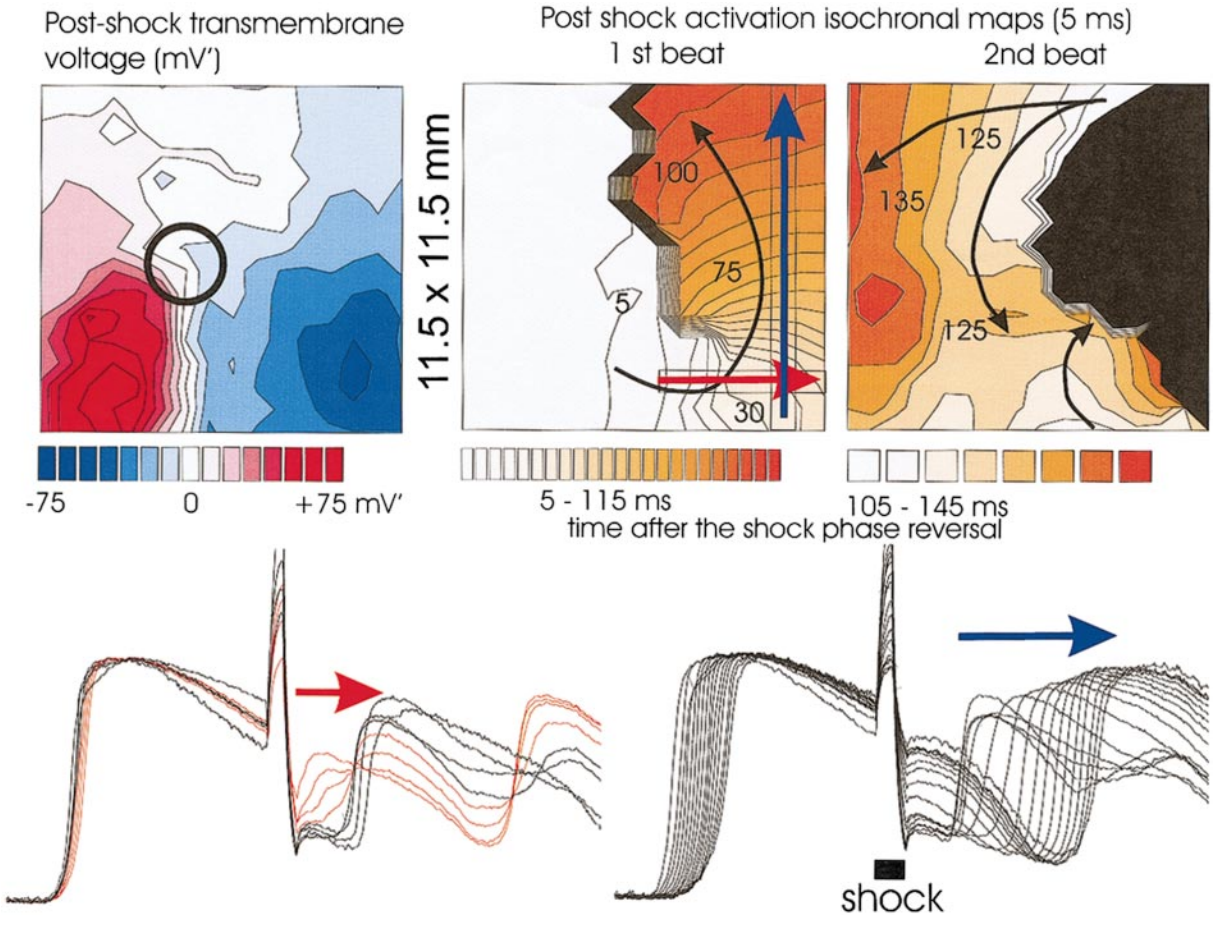

Figure 4. Creation of a shock-induced phase singularity. Electrical activity was recorded from the area shown in Figure 1 by the red box. The upper left panel shows the polarization pattern at the end of a +100/−200-V biphasic shock (15th millisecond of 16-ms shock), which resulted in a single extra beat. The scale is shown in millivolts, calibrated in the same manner described in Figure 1. The point of phase singularity is shown with the black circle. The upper middle panel shows a 5-ms isochronal map, which depicts the initiation of the postshock spread of activation. The map starts at the onset of the 8-ms second phase of the shock (phase reversal). The lower left and lower right panels show optical recordings from several recording sites used to reconstruct the activation maps: the eight sites marked with a red arrow correspond to the lower left panel, and the 16 sites marked with a blue arrow correspond to the lower right panel. The upper right panel shows a continuation of the reentrant activation that follows the middle panel. Reentrant activity then self-terminated, after encountering refractory tissue in the lower right corner of the field of view (see lower right panel traces).

The results shown in Figures 4 and 5 were confirmed in all 12 hearts. A total of 38 of 112 shocks resulted in extra beats and/or arrhythmias. Of these, 31 shocks were applied at 102±12 ms from the upstroke, and 7 shocks were applied at 50±7 ms from the upstroke.

The above data were obtained with shocks applied during the plateau phase of a normally propagating AP. In order to demonstrate that the same underlying mechanism is involved in defibrillation, we analyzed 19 unsuccessful defibrillation shocks (n=6 hearts). Fibrillation was induced by shocks applied as described before, during the plateau phase of the AP. Figure 6 shows the activation pattern recorded during one of these shocks. The lower left map shows the spread of activation during the last beat of VF, before the defibrillation attempt. Conduction was slow and emerged from several foci at the same time (white areas). Trace F (fluorescence) shows that during fibrillatory electrical activity, the transmembrane potential did not reach either full depolarization or resting potential; therefore, there was no excitable gap. Recordings in none of the 256 channels demonstrated the presence of an excitable gap. A cathodal monophasic shock (−150 V) produced a virtual electrode polarization pattern similar to the one shown in Figure 4, with positive polarization near the electrode and negative polarization on both sides (not shown). The middle activation map (isochrones 1 ms apart) shows that activation spread rapidly in the right half of the field of view, near the electrode. Then it spread to the left in the upper half, whereas it was blocked in the lower half. Activation then spread downward, completing the reentrant cycle. The point of phase singularity is shown with a red circle. Similar results, with clear evidence of the occurrence of a phase singularity followed by reentry, were observed in 14 of 19 unsuccessful defibrillation shocks. A phase singularity was also created in 2 of 12 successful defibrillation shocks. However, in these cases, reentry persisted for only one and three beats, respectively. If the postshock arrhythmias lasted more than three beats, the shock was considered unsuccessful. In two hearts, we were unable to defibrillate with any shocks, and these experiments were terminated.

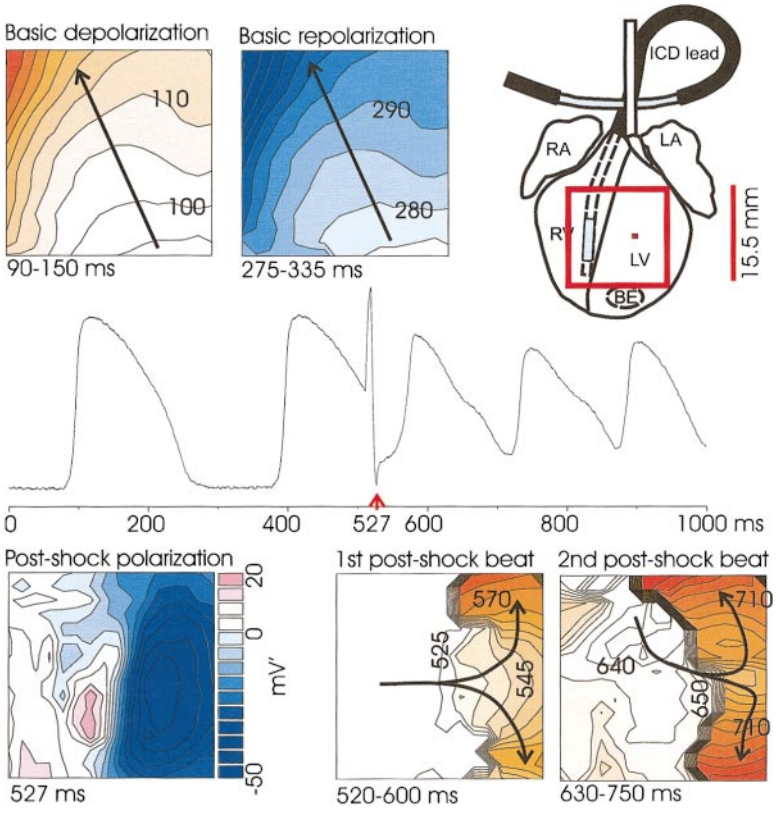

Figure 5. Pair of phase-singularity points produced by a +100/−170-V shock. The upper left and middle panels show activation and repolarization patterns of the basic beat, respectively. Time in all panels is given with respect to the beginning of the recording. The trace in the middle represents one recording from an LV site shown by a red box in the upper right panel. The lower left panel shows transmembrane polarization at the end of the shock (15th ms of 16-ms biphasic shock). Lower middle and right panels show 5-ms isochronal maps for the first and second reentrant beats, respectively. Time starts at the phase reversal (520 ms). RA and LA indicate right and left atrium, respectively.

Discussion

Lewis[15] suggested in 1925 that fibrillation has a reentrant nature and that the difference between fibrillation and tachycardia is that the reentrant pattern in tachycardia is repeated accurately, whereas in fibrillation it is not. Our findings demonstrate that in the rabbit heart VF may be initiated via the mechanism of virtual electrode–induced phase singularity. This leads to the creation of multiple reentrant circuits that compose the fibrillatory substrate. The failure to defibrillate in our experiments also occurred via the virtual electrode–induced phase-singularity mechanism.

Two main hypotheses have previously been proposed to explain the mechanisms of defibrillation: the CM hypothesis[16–18] and the ULV hypothesis.[19] The first hypothesis suggests that a critical amount of tissue is required to sustain fibrillation. Two underlying mechanisms have been proposed to support the CM hypothesis: statistical and dynamic. Both postulate that VF must be extinguished in a significant portion of the myocardium but that the remaining fibrillatory activity will self-terminate. The statistical CM hypothesis[20] postulates that a critical number of wavelets is required to sustain fibrillation, because of the statistical nature of their

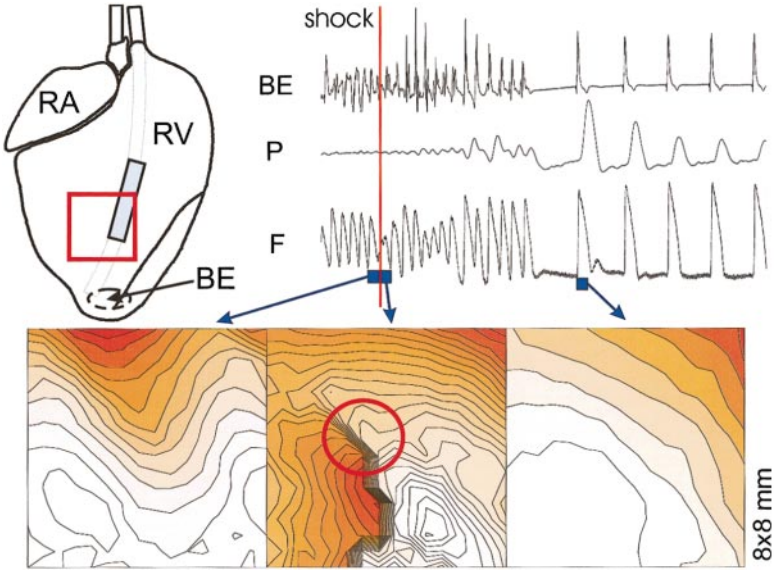

Figure 6. A phase singularity is produced during a failed defibrillation shock. Upper left panel shows the location of the field of view with respect to defibrillation electrode. Upper right panel shows the following: bipolar electrogram (BE), aortic pressure (P), and fluorescent signal (F) from one of the optical recording sites. Timing of the shock application is shown with the vertical thick line (shock). Lower maps show activation sequences (1-ms isochrones) just before the shock (left), immediately after the shock (middle), and after restoration of sinus rhythm (right). RA indicates right atrium.

birth and death.[17] The dynamic CM hypothesis is based on the observation that some critical amount of tissue is required to support even a single reentry, which may evolve indefinitely long in a nonstationary fashion if provided with sufficient space.[21,22] In contrast to these hypotheses, the ULV hypothesis postulates that VF must be extinguished everywhere throughout the heart. To succeed, a critical voltage gradient (named the upper limit of vulnerability) has to be reached everywhere in order to fully extinguish VF and not reinduce VF via a critical-point mechanism.[23] The primary area of disagreement between the two theories is not in the mechanism of defibrillation but in the understanding of the mechanisms of the failure to defibrillate.

The concept of virtual electrode–induced phase singularity was clearly visualized in our experiments. The map of transmembrane potential shown in the upper left panel of Figure 4 can be interpreted in terms of the phase of the electrical activity. Full depolarization shall be assigned phase $\phi=0$ but $\phi=2\pi$ if the full repolarization is reached. The transmembrane voltage shown can then be translated into a phase value by using additional information about dV/dt. The sign of dV/dt is needed to distinguish phases corresponding to the activation ($dV/dt>0$) from phases corresponding to the repolarization ($dV/dt<0$). The area marked with a black circle (Figure 4) contains a point that yields the mathematical definition of a phase singularity, known also as a critical point, which has been previously demonstrated to result in reentrant activity.[23]

However, the mechanism of creating phase singularities and reentry in the present study is significantly different from that in the critical point concept as described by Frazier et al.[23] Indeed, the repolarization map of the last basic beat, shown in the upper middle panel of Figure 5, shows that the repolarization gradient is directed from apex to base and that the polarization gradient is pointed from left to right. According to the critical point mechanism, one would expect only the upper phase singularity to be formed by the shock, because this is the only site at which an appropriate cross-field pattern between repolarization and electric field gradients is formed. The lower phase singularity cannot be explained by the critical-point mechanism and therefore provides compelling evidence of the novelty of our finding.

Our data indicate that the phase-singularity mechanism is indeed involved in electrical activity resulting from proarrhythmic ICD shocks. However, point singularities resulted in self-sustained arrhythmias (>3 minutes) in only 10.7% of cases (12 of 112), whereas the remaining reentries self-terminated. In 24 cases we could clearly identify that the reentrant wave front propagated along a line of conduction block, turned around a pivoting point, and then self-terminated by encountering refractory tissue (see the example in Figure 4). Therefore, the arrhythmia may halt spontaneously, as according to the CM hypothesis. However, it is important to note that our data cannot clearly identify which is the correct theory, because we did not look at the nonextinguished preshock fibrillatory electrical activity, and we could not map the electrical activity of the entire heart.

Both the CM and the ULV theories have their limitations. The CM theory does not specify exactly how the remaining VF will self-terminate, whereas the ULV theory fails to recognize the difference between depolarizing and hyperpolarizing voltage gradients and especially the boundaries between them. These boundaries are associated with the creation of phase singularities and may occur close to the electrodes, not far away, as postulated by the ULV hypothesis. Furthermore, neither hypothesis specifies exactly how fibrillatory electrical activity is extinguished at the cellular level.

Several basic mechanisms have been proposed to explain defibrillation at the cellular level: (1) prolongation of AP duration[6] and refractoriness,[24,25] known also as graded responses,[26] and (2) reactivation of sodium channels[27] with possible subsequent break excitation.[14]

Our optical data indicate that nearly all of these effects may be involved in defibrillation, at the same time, in different parts of the heart, in which extracellular field gradients of opposite polarity produce either inward or outward current sources. However, our data demonstrate that the success of the shock is related not solely to the degree of AP prolongation but rather to the homogeneity of postshock transmembrane polarization. Indeed, Figure 1 indicates that shocks that resulted in no postshock extra beats or arrhythmias prolonged the AP least of all (see green traces). Thus, their defibrillation efficacy is more likely related to the homogenization of the postshock phase distribution, because strong phase gradients may produce propagated responses via the break excitation mechanism.[14] The latter can form a reentrant circuit if a phase singularity is created in addition to the phase gradient.

Numerous basic and clinical studies have empirically identified certain monophasic and biphasic defibrillation waveforms that are relatively more efficient than others.[28–30] Our data support a logical explanation for why a specific waveform may be better than others. We have shown that if the ratio between the leading-edge voltage of the second phase and that of the first phase is in the range of 0.2 to 0.7, then the shock creates a relatively homogeneous postshock transmembrane polarization and phasic pattern with no substrate for creating points of phase singularity. Therefore, we suggest that these waveforms will be the least likely to induce postshock arrhythmias via the virtual electrode–induced phase-singularity mechanism. Our results are consistent with defibrillation threshold measurements in humans.[31]

The present study has several limitations. Mapping of electrical activity was confined to only a limited epicardial area. Therefore, we may have missed the induction of some other phase singularities that may have occurred beyond our field of view and at the endomyocardium and midmyocardium. Asynchronous measurements indicated that phase singularities are likely to occur at four sites around the RV electrode in areas where negative, positive, and no polarization meet. This is qualitatively similar to the theoretical prediction of Roth and Saypol,[32] who proposed the involvement of a VEP in the proarrhythmic response to a premature pacing stimulus applied at the vulnerable period of an AP. Their hypothesis was based on the interaction of stimulus-induced virtual electrode polarization and the preshock phase pattern. Our data indicate that a strong shock may overcome the preshock electrical activity and create phase singularities,

regardless of the preshock phase distribution (see Figure 4). Furthermore, unlike low-energy pacing, defibrillation shocks create VEPs comparable to the size of the heart. Therefore, additional areas of opposite polarization may be present, for example, at the septum. Thus, additional phase singularities may be generated.

The present study does not address the issue of the three-dimensional pattern of polarization. We can record averaged electrical activity from only a 500-μm superficial layer of the epicardium.[33] However, our findings can be easily extended to a three-dimensional case. Reversal of negatively polarized areas should be easier than reversal of positively polarized patterns, presumably because of the involvement of different ionic currents at different levels of transmembrane polarization and therefore different levels of transmembrane impedance to the polarizing effects of the shock. Postshock propagation from depolarized to negatively polarized areas must occur in the three-dimensional case as well. The exact three-dimensional organization of the propagation pattern remains to be elucidated, perhaps by use of a bidomain simulation approach. Recent findings (E. Entcheva, J. Eason, I.R. Efimov, Y. Cheng, R.A. Malkin, F. Claydon, unpublished data, 1998) indicate that two-dimensional phase singularities and vortices in three dimensions may correspond to filaments of phase singularity and twisted and curved scrolls, respectively. The twisted shape of the filament is a result of the rotation of fiber orientation within the ventricular wall. Detection of the VEP on the epicardium suggests that these scrolls are likely to be transmural and therefore may evolve into stable three-dimensional sources of reentrant activity, as has been shown in mathematical simulations.[10]

References

1. Prevost JL, Battelli F. Sur quelques effets des décharges électriques sur le coeur des mammifères. *Comptes Rendus Séances Acad Sci*. 1899;129: 1267.
2. Beck CS, Pritchard WH, Feil HS. Ventricular fibrillation of long duration abolished by electric shock. *JAMA*. 1947;135:985–986.
3. Zoll PM, Linethal AJ, Gibson W, Paul MH, Norman LR. Termination of ventricular fibrillation in man by externally applied electric shock. *N Engl J Med*. 1956;254:727–732.
4. Mirowski M, Mower MM, Staewen WS, Tabatznik B, Mendeloff AI. Standby automatic defibrillator: an approach to prevention of sudden coronary death. *Arch Intern Med*. 1970;126:158–161.
5. Schuder JC, Stoeckle H, Gold JH, West JA, Keskar PY. Experimental ventricular defibrillation with an automatic and completely implanted system. *Trans Am Soc Artif Intern Organs*. 1970;16:207–212.
6. Dillon SM. Optical recordings in the rabbit heart show that defibrillation strength shocks prolong the duration of depolarization and the refractory period. *Circ Res*. 1991;69:842–856.
7. Zhou X, Ideker RE, Blitchington TF, Smith WM, Knisley SB. Optical transmembrane potential measurements during defibrillation-strength shocks in perfused rabbit hearts. *Circ Res*. 1995;77:593–602.
8. Efimov IR, Cheng YN, Biermann M, Van Wagoner DR, Mazgalev TN, Tchou PJ. Transmembrane voltage changes produced by real and virtual electrodes during monophasic defibrillation shock delivered by an implantable electrode. *J Cardiovasc Electrophysiol*. 1997;8:1031–1045.
9. Wiener N, Rosenblueth A. The mathematical formulation of the problem of conduction of impulses in a network of connected excitable elements, specifically in cardiac muscle. *Arch Inst Cardiol Mex*. 1946;16:205–265.
10. Winfree AT. *When Time Breaks Down: The Three-Dimensional Dynamics of Electrochemical Waves and Cardiac Arrhythmias*. Princeton, NJ: Princeton University Press; 1987:125–153.
11. Frazier DW, Wolf PD, Wharton JM, Tang AS, Smith WM, Ideker RE. Stimulus-induced critical point: mechanism for electrical initiation of reentry in normal canine myocardium. *J Clin Invest*. 1989;83:1039–1052.
12. Salama G, Kanai A, Efimov IR. Subthreshold stimulation of Purkinje fibers interrupts ventricular tachycardia in intact hearts: experimental study with voltage-sensitive dyes and imaging techniques. *Circ Res*. 1994;74:604–619.
13. Efimov IR, Huang DT, Rendt JM, Salama G. Optical mapping of repolarization and refractoriness from intact hearts. *Circulation*. 1994;90: 1469–1480.
14. Roth BJ. A mathematical model of make and break electrical stimulation of cardiac tissue by a unipolar anode or cathode. *IEEE Trans Biomed Eng*. 1995;42:1174–1184.
15. Lewis T. *The Mechanism and Graphic Registration of the Heart Beat.* London, UK: Shaw and Sons Ltd; 1925.
16. Garrey WE. The nature of fibrillary contraction of the heart: its relations to tissue mass and form. *Am J Physiol*. 1914;33:397–414.
17. Krinskii VI, Fomin SV, Kholopov AV. Critical mass during fibrillation [in Russian]. *Biofizika*. 1967;12:908–914.
18. Zipes DP, Fischer J, King RM, Nicoll A deB, Jolly WW. Termination of ventricular fibrillation in dogs by depolarizing a critical amount of myocardium. *Am J Cardiol*. 1975;36:37–44.
19. Chen PS, Shibata N, Dixon EG, Martin RO, Ideker RE. Comparison of the defibrillation threshold and the upper limit of ventricular vulnerability. *Circulation*. 1986;73:1022–1028.
20. Moe GK. A conceptual model of atrial fibrillation. *J Electrocardiol*. 1968;1:145–146.
21. Zykov VS. Cycloidal circulation of spiral waves in excitable medium [in Russian]. *Biofizika*. 1986;31:862–865.
22. Efimov IR, Krinsky VI, Jalife J. Dynamics of rotating vortices in the Beeler-Reuter model of cardiac tissue. *Chaos Solitons Fractals*. 1995;5: 513–526.
23. Frazier DW, Wolf PD, Wharton JM, Tang AS, Smith WM, Ideker RE. Stimulus-induced critical point: mechanism for electrical initiation of reentry in normal canine myocardium. *J Clin Invest*. 1989;83:1039–1052.
24. Swartz JF, Jones JL, Jones RE, Fletcher R. Conditioning prepulse of biphasic defibrillator waveforms enhances refractoriness to fibrillation wavefronts. *Circ Res*. 1991;68:438–449.
25. Sweeney RJ, Gill RM, Reid PR. Characterization of refractory period extension by transcardiac shock. *Circulation*. 1991;83:2057–2066.
26. Kao CY, Hoffman BF. Graded and decremental responses in heart muscle fibers. *Am J Physiol*. 1958;194:187–196.
27. Jones JL, Jones RE, Milne KB. Refractory period prolongation by biphasic defibrillator waveforms is associated with enhanced sodium current in a computer model of the ventricular action potential. *IEEE Trans Biomed Eng*. 1994;41:60–68.
28. Walcott GP, Walcott KT, Knisley SB, Zhou X, Ideker RE. Mechanisms of defibrillation for monophasic and biphasic waveforms [review]. *Pacing Clin Electrophysiol*. 1994;17:478–498.
29. Shorofsky SR, Foster AH, Gold MR. Effect of waveform tilt on defibrillation thresholds in humans. *J Cardiovasc Electrophysiol*. 1997;8: 496–501.
30. Huang J, KenKnight BH, Walcott GP, Walker RG, Smith WM, Ideker RE. Effect of electrode polarity on internal defibrillation with monophasic and biphasic waveforms using an endocardial lead system. *J Cardiovasc Electrophysiol*. 1997;8:161–171.
31. Feeser SA, Tang AS, Kavanagh KM, Rollins DL, Smith WM, Wolf PD, Ideker RE. Strength-duration and probability of success curves for defibrillation with biphasic waveforms. *Circulation*. 1990;82:2128–2141.
32. Roth BJ, Saypol JM. The formation of a re-entrant action potential wave front in tissue with unequal anisotropy ratios. *Int J Bifurc Chaos*. 1991; 4:927–928.
33. Girouard SD, Laurita KR, Rosenbaum DS. Unique properties of cardiac action potentials recorded with voltage-sensitive dyes. *J Cardiovasc Electrophysiol*. 1996;7:1024–1038.